

Low-energy nonresonant x-ray scattering of C_{60}

Paul Chow

HPCAT, Geophysical Laboratory, Carnegie Institution of Washington, Building 434E, 9700 South Cass Avenue, Argonne, Illinois 60439, USA

Barry Friedman

Physics Department, Sam Houston State University, Huntsville, Texas 77341-2267, USA

(Received 8 August 2007; revised manuscript received 18 December 2007; published 25 February 2008)

Using a third generation synchrotron, the low-energy electronic structure of C_{60} was measured by nonresonant inelastic x-ray scattering. The cross section $S(k, \omega)$ at $k=1.0 \text{ \AA}^{-1}$ reveals a significant peak at 2.1 eV inaccessible to optical absorption due to selection rules but consistent with measurements done by nonlinear optics and electron energy-loss spectroscopy. The experiment was modeled by a Hubbard model for a single C_{60} molecule with $U/t=4$. This simple model captures the essential physics.

DOI: [10.1103/PhysRevB.77.073406](https://doi.org/10.1103/PhysRevB.77.073406)

PACS number(s): 71.10.Fd, 78.30.Na, 78.70.Ck

To properly understand superconductivity and other collective effects in fullerene systems, it is essential to develop simple models of their low-energy electronic structure and compare direct consequences of these models against experimental results. Electron doped C_{60} with maximum superconducting critical temperatures greater than 30 K (Ref. 1) is a particularly interesting system to investigate. Over 15 years ago, it was proposed that a simple tight binding model for the π electrons,² augmented with an on-site Hubbard repulsion U ³ is adequate to explain C_{60} 's low-energy electronic properties.⁴ In such a model, described in more detail below, two nondegenerate energy levels at approximately 3.0 eV in the noninteracting model are split by the repulsive Hubbard U to roughly 3.0 and 3.6 eV. These energy levels are dipole allowed, and hence observable through optical absorption. Optical absorption gives a small peak at 3.0 eV and a large peak at 3.6 eV corresponding to the calculated energy levels.^{4,5} The ratio of the strengths of the absorption peaks is in reasonable agreement with calculations where a Hubbard U of approximately $4t$ is chosen. Here, t is the transfer integral between nearest neighbor carbon atoms on the C_{60} molecule. The total bandwidth of the π energy levels of the C_{60} molecule is approximately $6t$. Such a Hubbard U puts C_{60} in the regime of strong but not exceeding strong (for example, $U > 10t$ in the cuprates⁶) effective electron-electron interaction. This is the size of Hubbard U typically invoked in conducting polymer systems.⁷ It is important to note that these optical absorption experiments can be understood by models in which the intermolecular electron transfer between C_{60} molecules (i.e., one only need consider a single C_{60} molecule) is not taken into account. This is justified because the hopping between molecules is much smaller than the intramolecular transfer. Experimentally, this is supported by the fact that the optical absorption spectra of C_{60} done on the C_{60} solid and in solution are quite similar. There have been several recent theoretical investigations where the issue of electron correlation in C_{60} plays an important role.⁸⁻¹⁰ In particular, by setting $U=4t$, the authors of Ref. 10 have found agreement with x-ray photoemission diffraction experiments.¹¹ To obtain this agreement, parameters describing a rotation angle and intermolecular hopping of electrons between C_{60} molecules were fitted to experiment. Due to

limitations in computer time, U was not fitted (i.e., a plausible value $U=4t$ was chosen). Hence, it is of some current interest to verify the value of U by other experimental means.

Clearly, linear optical techniques are important and serve as simple methods to characterize the electronic structure of C_{60} . However, optical absorption, due to the high symmetry of the C_{60} molecule, could possibly "miss" energy levels due to selection rules. A way around this limitation is to use nonlinear optical techniques but the interpretation and implementation of these methods may not be straightforward or unambiguous.¹² In addition to optical techniques, the electronic structure of C_{60} has been investigated using electron energy-loss spectroscopy (EELS).^{13,14} This technique is not constrained by selection rules but possible limitations include multiple scattering and surface effects. Another attractive approach, which could potentially yield additional information, is (nonresonant) inelastic x-ray scattering (IXS). In optical absorption, the scattering function $S(k, \omega)$ at approximately zero momentum transfer k is observed as a function of energy transfer ω . One is limited to zero momentum transfer in optical techniques due to the small momentum of optical photons; however, for x rays, one is subject to no such limitation. Hence, in IXS, one can measure $S(k, \omega)$ for non-zero momentum transfers. This allows one to probe dipole forbidden states. More broadly speaking, probing at different k gives one the ability to probe different length scales as well as energy scales.^{15,16} One particularly noteworthy feature of IXS is that if the experiment can be done, the interpretation is straightforward, as one is measuring $S(k, \omega)$ without any complications due to multiple scattering or surface effects. Unfortunately, the scattering cross section for IXS is generally quite small and, thus, experiments are difficult. However, C_{60} is an ideal material for IXS in that Z , the atomic number of carbon, is low, suppressing absorption of the x rays and the development of extremely intense third generation synchrotrons has broadened the range of possible experiments. The most intense features of $S(k, \omega)$ of C_{60} , the plasmons of energy roughly 30 eV and a peak at approximately 5 eV, have already been observed some time ago with low-energy resolution.¹⁷ The third generation synchro-

trons, for example, SPring-8, near Himeji, Japan, have opened the possibilities of high-resolution studies (70 meV) at relatively low-energy transfer, 1–5 eV, avoiding the elastic line for “favorable” momentum transfers. We have therefore undertaken a combined experimental and theoretical study of the electronic properties of C_{60} using IXS.

The Hamiltonian chosen to describe the C_{60} molecule consists of a tight binding model for the 60 π electrons with on-site Hubbard repulsion:

$$H = \sum_{s(ij)} -t_{ij}(c_{is}^+c_{js} + c_{js}^+c_{is}) + U \sum_i n_{i\uparrow}n_{i\downarrow}, \quad (1)$$

c_{is} , c_{is}^+ being electron creation and annihilation operators and $n_{is} = c_{is}^+c_{is}$. The σ electrons, other than their influence on the effective parameters U and t_{ij} , have been neglected and the long range Coulomb repulsion has been replaced by an on-site Hubbard term. Both these approximations appear to be adequate for the low-energy optical properties, though inadequate to describe the higher-energy plasmons. The aim here is to establish the simplest model to describe the low energy optical and inelastic x-ray scattering experiments. Likewise, the transfer between molecules has been ignored. For the parameters t_{ij} , a standard value $t=2.5$ eV for hopping along a single bond separating a pentagon and a hexagon has been used, while for hopping along a shorter double bond separating two hexagons, $t_{ij}=t+0.1t$. A Hubbard U of 10 eV gives good agreement with the low-energy optical absorption experiments; in essence, U is “fitted” by these experiments.

To calculate optical absorption or IXS, one needs to be able to calculate the ground state and low lying excited states of the Hamiltonian. Unfortunately, despite the apparent simplicity of the model, this is a quite daunting task, the reason being that there are 60 interacting electrons. A brute force calculation would require finding the low lying eigenstates of a matrix having dimension $(60!/30!30!)^2 \cong 1.4 \times 10^{34}$ [by spin rotation invariance of the Hamiltonian, it is sufficient to consider the case of 30 spin up electrons and 30 spin down electrons, i.e., $(60!/30!30!)$, being the number of ways of putting 30 spin up electrons in 60 orbitals]. Therefore, a tractable approximation or truncation procedure is necessary. The simplest approximation scheme that can do a reasonable job at calculating optical absorption is one-particle configuration interaction (CI). One-particle CI is a truncation of state space done by including the lowest-energy noninteracting state (fill the 30 lowest-energy single-particle states, the “Fermi” sea) and all states accessible from this state by creating one particle-hole pair. The state space has thus been reduced from an intractable 1.4×10^{34} to a tractable $30 \times 30 \times 2 + 1 = 1801$ states. By working in this truncated state space, the many-electron ground state and all the excited states can be obtained by a straightforward numerical diagonalization.

To calculate the cross section for IXS, it is necessary to evaluate the expression

$$S(k, \omega) = \sum_{n_1} |\langle n_1 | \sum_j e^{ik \cdot r_j} | G \rangle|^2 \delta(E_G - E_{n_1} + \hbar\omega). \quad (2)$$

Here, k and ω are the momentum and energy transfer, $\langle n_1 |$ are excited states, and $|G\rangle$ is the ground state. For a C_{60}

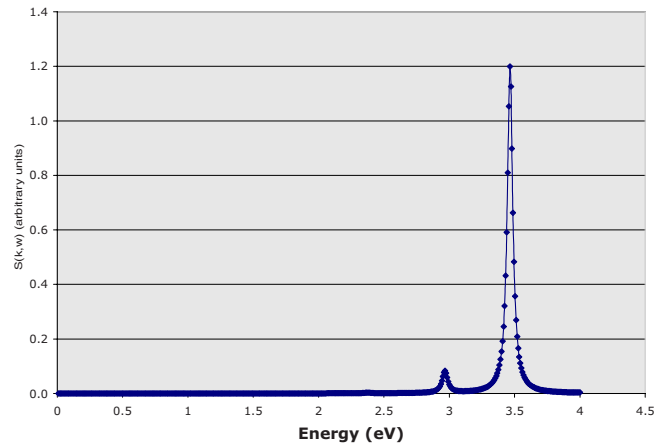


FIG. 1. (Color online) Calculated $S(k, \omega)$ vs energy ($\hbar\omega$) for $k=0.1 \text{ \AA}^{-1}$.

molecule, the ground state is separated by greater than an eV from excited states so one needs only consider excitation from the ground state. The r_j are coordinates of the π electrons and the sum runs over all 60 π electrons. Within the single CI approximation, all the excited states are known and this expression can be easily evaluated numerically. The cross section for IXS is proportional to Eq. (2), the constant of proportionality not being important for our purposes, as we will only be concerned with the energy loss and relative strength of peaks. In the actual calculation, the delta function has been replaced by a Lorentzian of width Γ . This choice is made for simplicity and is not intended to have physical significance. The actual physical peak shape observed in IXS contains important information but is beyond the scope of the present simple theoretical considerations.

Let us now turn to the results of calculations of $S(k, \omega)$ for low energy and differing magnitudes of k . In Fig. 1, $S(k, \omega)$ for a small value of $k=0.1 \text{ \AA}^{-1}$ has been plotted. A width of $\Gamma=.05$ eV has been used and the orientation of the C_{60} molecule has been averaged over. Due to the symmetry of the C_{60} molecule, this averaging has a minor effect. Since k is small, $k=0.1 \text{ \AA}^{-1}$, $\lambda=2\pi/k \approx 63 \text{ \AA}$ with the diameter of the C_{60} molecule being about 7 \AA ; the results are quite similar to optical absorption; there is a small peak at 3 eV and a large peak at 3.5 eV. These results are consistent with (though not in “perfect” agreement) experiment. Of course, perfect agreement should not be expected, i.e., one-particle CI is not an exact calculation, the σ electrons have been neglected, etc. Figure 2 illustrates what happens as k increases; $S(k, \omega)$ for $k=0.5 \text{ \AA}^{-1}$ has been plotted. The most interesting feature of Fig. 2 is the presence of a small new peak at 2.4 eV. What happens to this peak as k is increased further? Figure 3 is a graph of $S(k, \omega)$ for $k=1.0 \text{ \AA}^{-1}$. The relative height of the 2.4 eV peak has grown significantly in comparison to the large peak at 3.5 eV. The simple single CI calculation thus makes an unambiguous prediction as k increases: a peak not present in optical absorption will appear at roughly 2.4 eV. The peak appears where the model is at its best and relatively low energy, and there are no free parameters. This peak should be of a “comparable” size to the peak at 3.5 eV at $k=1.0 \text{ \AA}^{-1}$.

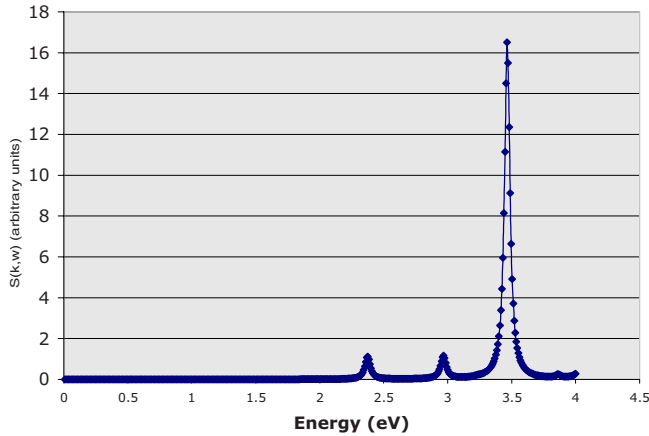


FIG. 2. (Color online) Calculated $S(k, \omega)$ vs energy for $k = 0.5 \text{ \AA}^{-1}$.

Let us now briefly consider our experimental setup. In broad outline, incident monochromatic photons impinge on the sample and scatter from its electrons, and the photon energy loss and momentum transfer are measured. The scattering cross section yields information about the corresponding energy and momentum gain of the electron system. IXS measurements on C_{60} were performed on beamline BL12XU Spring-8, Japan, using a Si(111) pair of crystals in the double crystal monochromator and a Si(333) pair of channel cuts for the high-resolution monochromator. The spectrometer employed three 100 mm Si(555) diced 2 m radius analyzers in vertical geometry, giving an overall energy resolution of about 70 meV in the near-backscattering mode at the elastic energy of 9884.92 eV. The sample in vacuum was 2.5 mm thick powdered C_{60} (Johnson Matthey Japan, No. 42008 fullerene powder, sublimed, 99.995%) sandwiched by a 2.5 μm thick Mylar film on either side. A monochromatic Laue photograph revealed a textured powder, as expected. Due to the relaxed k resolution ($\pm 0.12/\text{\AA}$ from the analyzer array in order to reduce counting times) and Bragg peaks from the crystalline structure, the C_{60} energy-loss spectra of certain q values were not measurable because of the long tails of the elastic line. A different portion of the sample was exposed to the incident x rays for each scan in case of beam damage. After verifying the overall shape of the energy-loss

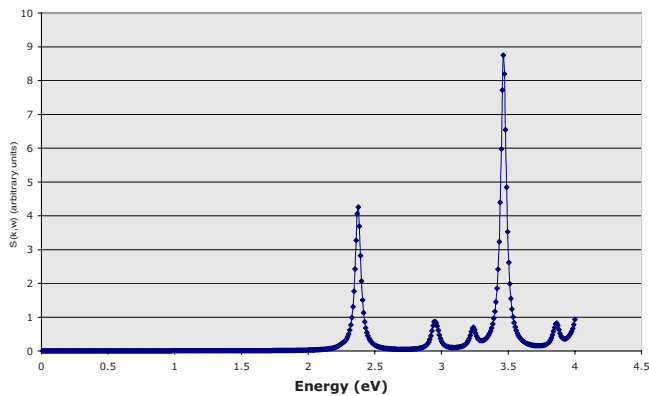


FIG. 3. (Color online) Calculated $S(k, \omega)$ vs energy for $k = 1.0 \text{ \AA}^{-1}$.

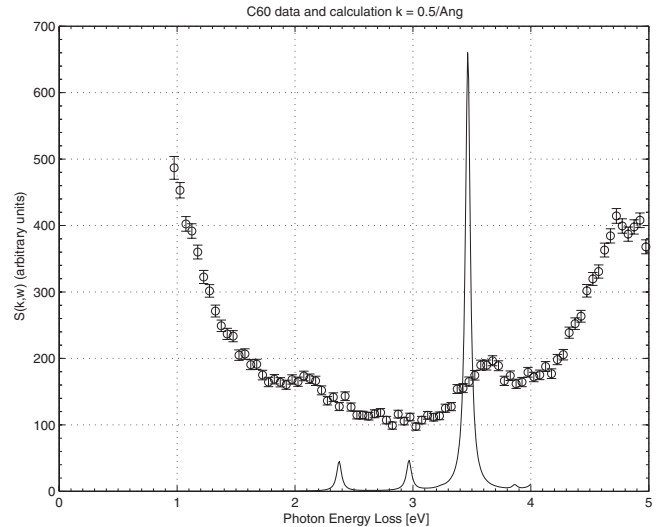


FIG. 4. Measured $S(k, \omega)$ vs energy for $k = 0.5 \text{ \AA}^{-1}$. The calculation is also included in the figure.

spectrum, including plasmons, we concentrated on the optical region of 1–5 eV energy loss at moderate k values to compare with the model calculations. The high-energy resolution of the spectrometer was necessary to resolve the features in this part of the spectrum.

The results of the experiment, together with the previously described calculations, are displayed in Figs. 4 and 5. Figure 4 (5) is a plot of $S(k, \omega)$ vs photon energy loss for $k = 0.5 \text{ \AA}^{-1}$ (1.0 \AA^{-1}). In the lower k measurement (Fig. 4), one sees peaks at 3.7 and 2.1 eV. The existence of a transition at 2.1 eV is consistent with nonlinear optical spectroscopy¹² and EELS.^{13,17} The peak at 3.7 is more intense than the 2.1 eV peak. However, due to the tail of the elastic line, which is pronounced at this momentum transfer, it is difficult to draw any quantitative conclusion about the relative height of the peaks. Qualitatively, however, the 3.7 eV peak is

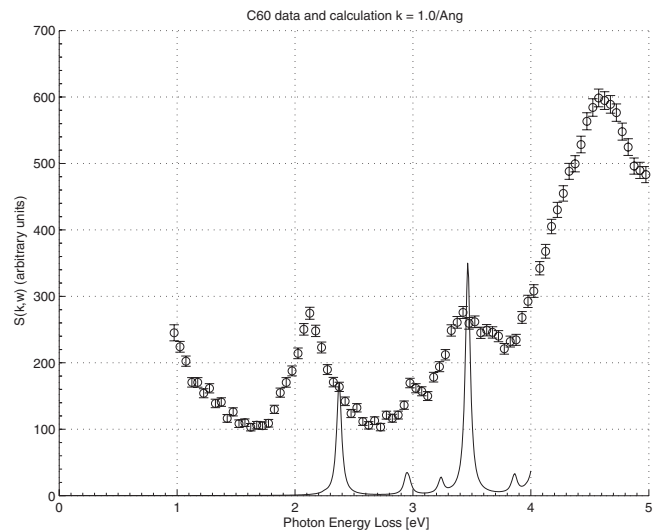


FIG. 5. Measured $S(k, \omega)$ vs energy for $k = 1.0 \text{ \AA}^{-1}$. The calculation is also included in the figure.

larger and is substantially larger, assuming a rapid decay of the elastic line starting at about 1.8 eV. This is compared to the calculations that give a larger peak at 3.5 eV and much smaller peaks at 3.0 and 2.4 eV. Again, we emphasize that the width of the theoretical peaks has no physical significance in our calculations.

Turning now to the higher k measurement (Fig. 5), a weak feature has emerged at 3 eV and the relative strength of the 2.1 eV peak has increased compared to the peak at 3.5 eV (the 3.7 eV peak has shifted to 3.5 eV). We make a provisional identification of the weak feature at 3 eV with the peak observed at 3 eV in optical absorption experiments.⁵ A noticeable and helpful feature of this measurement is a weaker strength of the elastic line in the energy region of interest. The most significant discrepancy between experiment and theory is the position of the 2.1 eV peak, which, in the calculation, takes a value of 2.4 eV. This happens at relatively low energies where a π electron model should be most reliable; hence, it is tempting to attribute this difference to a “higher order” correlation effect, that is, the inadequacy of one-particle CI. However, the elastic tails are larger in this region, compared to 3 or 3.5 eV, and the subtraction of the elastic tail could affect the peak position.

Since we do not know a consistent way to subtract the elastic peak and we do not have a theory of the peak shape, it is difficult to compare the measured peak ratios to the calculation. However, if one subtracts a cross section of 100 from the 2.1 eV peak and nothing from the 3.5 eV peak, one gets an intensity ratio of 1.5 compared to a theoretical ratio of roughly 2. Again, due to the ambiguities involved, the significance of this disagreement is difficult to access. In any case, experiment and theory appear to be in semiquantitative agreement.

Measurement of the dynamic structure factor $S(k, \omega)$ is

related to the imaginary part of the inverse dielectric function $\varepsilon(k, \omega)$ and gives information on the response of an electron system to perturbations. $S(k, \omega)$ can also be interpreted in terms of electronic excitations. In this Brief Report, using a third generation synchrotron, we were able to investigate the low-energy electronic structure of C_{60} by inelastic x-ray scattering, relating $S(k, \omega)$ to the underlying microscopic interactions of electrons of the model Hamiltonian. The cross section at $k=1.0 \text{ \AA}^{-1}$ reveals a significant peak at 2.1 eV inaccessible to optical absorption due to selection rules but consistent with measurements done by nonlinear optics and EELS. Our experimental results were modeled by a Hubbard model for a single C_{60} molecule with $U/t=4$ solved within the single-particle CI approximation. Most importantly, this simple model predicts, in agreement with experiment, that a significant low-energy peak should appear as the momentum transfer k increases. This agreement verifies¹⁴ that the peak at 2.1 eV is a single molecule effect. It appears possible and of interest to apply a similar theoretical approach and experimental methods to study the electronic structure of other organic materials, for example, conducting polymers and doped fullerene systems.

This work was supported in part by the NSF through Grant No. DMR-0307170. Portions of this work were performed at BL12XU SPring-8 and HPCAT (Sector 16), Advanced Photon Source (APS), Argonne National Laboratory. The work at BL12XU SPring-8 was partly supported by the National Science Council of Taiwan. Use of the HPCAT facility was supported by DOE-BES, DOE-NNSA (CDAC), NSF, DOD-TACOM, and the W.M. Keck Foundation. Use of the APS was supported by DOE-BES under Contract No. W-31-109-ENG-38.

¹A. P. Ramirez, *Supercond. Rev.* **1**, 1 (1994).

²V. Elser and R. C. Haddon, *Phys. Rev. A* **36**, 4579 (1987).

³B. Friedman and Jaewan Kim, *Phys. Rev. B* **46**, 8638 (1992).

⁴M. I. Salkola, *Phys. Rev. B* **49**, 4407 (1994).

⁵S. L. Ren *et al.*, *Appl. Phys. Lett.* **59**, 2678 (1991).

⁶E. Dagotto, *Rev. Mod. Phys.* **66**, 763 (1994).

⁷A. J. Heeger, S. Kivelson, J. R. Schrieffer, and W. P. Su, *Rev. Mod. Phys.* **60**, 781 (1988).

⁸F. Lin, J. Smakov, E. S. Sorensen, C. Kallin, and A. J. Berlinsky, *Phys. Rev. B* **71**, 165436 (2005).

⁹G. P. Zhang and T. F. George, *Phys. Rev. B* **76**, 085410 (2007).

¹⁰F. Lin, E. S. Sorensen, C. Kallin, and A. J. Berlinsky, *Phys. Rev. B* **75**, 075112 (2007).

¹¹W. L. Yang *et al.*, *Science* **300**, 303 (2003).

¹²A. M. Janner, H. T. Jonkman, and G. A. Sawatzky, *Phys. Rev. B* **63**, 085111 (2001).

¹³H. Romberg, E. Sohmen, M. Merkel, M. Knupfer, M. Alexander, M. S. Golden, R. Adelman, T. Pietrus, J. Fink, R. Seeman, and R. L. Johnson, *Synth. Met.* **55-57**, 3038 (1993).

¹⁴M. Knupfer and J. Fink, *Phys. Rev. B* **60**, 10731 (1999).

¹⁵M. Knupfer, T. Pichler, M. S. Golden, J. Fink, M. Murgia, R. H. Michel, R. Zamboni, and C. Taliani, *Phys. Rev. Lett.* **83**, 1443 (1999).

¹⁶V. Chernyak, S. N. Volkov, and S. Mukamel, *Phys. Rev. Lett.* **86**, 995 (2001).

¹⁷E. D. Isaacs, P. M. Platzman, P. Zschack, K. Hamalainen, and A. R. Kortan, *Phys. Rev. B* **46**, 12910 (1992).